METEOROLOGICAL APPLICATIONS
Meteorol. Appl. **19**: 152–160 (2012)
Published online in Wiley Online Library
(wileyonlinelibrary.com) DOI: 10.1002/met.1332

RMetS
Royal Meteorological Society

Evaluation of upper tropospheric humidity from NCEP analysis and WRF Model Forecast with Kalpana observation during Indian summer monsoon 2010

Prashant Kumar, Munn V. Shukla,* Pradeep K. Thapliyal, Jagat H. Bisht and P. K. Pal
Atmospheric and Oceanic Sciences Group, Space Applications Centre (ISRO), Ahmedabad, India

ABSTRACT: This paper presents an evaluation of upper tropospheric humidity (UTH) fields from National Center for Environmental Prediction (NCEP) Global Data Assimilation System (GDAS) analysis and Weather Research and Forecasting (WRF) mesoscale model forecast with satellite derived UTH. For this purpose, UTH (weighted average of relative humidity in 200–500 hPa layer) obtained from Indian geostationary satellite Kalpana is compared with the UTH computed from NCEP analysis and WRF model forecast during the summer monsoon, 2010. Kaplana-derived products are not included in the NCEP analysis: therefore, a comparison of the two independent datasets is promising. This study indicates that UTH derived from different sources (Kalpana UTH, NCEP Analysed and subsequent model forecasted UTH) matches very well over the Indian region. However, there are region-specific small departures in UTH which increases the model predicted UTH. Copyright © 2012 Royal Meteorological Society

KEY WORDS Upper Tropospheric Humidity; Kalpana; WRF Model; NCEP analysis

Received 19 December 2011; Revised 8 April 2012; Accepted 23 April 2012

1. Introduction

It is widely recognized that information about atmospheric water vapour in general and upper troposphere humidity in particular is very important for both climate and numerical weather prediction (NWP) applications (Soden and Bretherton, 1993; Salathé *et al*., 1995; McNally *et al*., 1996; Bates *et al*., 1996; Blackwell and McGuirk, 1996; Macpherson *et al*., 1996). The accurate estimation of water vapour is even more important in the tropical region than any other geographical region. In the tropical regions the water vapour is highly variable and is dominated by deep convective systems (Brown and Zhang, 1997) leading to increased relative humidity in the upper troposphere (Soden and Fu, 1995). Observations of the UTH could help in the diagnosing convective processes in the atmospheric model simulations.

The Indian summer monsoon, which is highly influenced by mesoscale convective systems, provides the best test-bed for any model diagnostics. The NWP models are mainly initial value problems. Therefore, they are highly dependent on accurate data regarding the initial atmospheric state. The initial atmospheric fields used in mesoscale models are taken from the analysis generated from global circulation models (GCMs). Therefore, for better diagnostics of the model simulations it is required that the initial atmospheric fields must be consistent with the actual atmospheric state. Atmospheric humidity is one of the important parameters of initial atmospheric fields, which can be used for this purpose. Various studies have been performed to evaluate the analysed (Clark and Harwood, 2003; Lamquin *et al*., 2008) and model forecasted (Schmetz and Berg, 1994) UTH with observed UTH. Recently, Dessler and Davis (2010) compared tropospheric humidity generated from various reanalysis: Japanese Reanalysis (JRA) (Onogi *et al*., 2007), the NASA Modern Era Retrospective-Analysis for Research and Applications (MERRA) (Suarez *et al*., 2008), European Centre for Medium Range Weather Forecasts (ECMWF) interim reanalysis (Simmons *et al*., 2007), ERA40 (Uppala *et al*., 2005) and NCAR reanalysis (Kalnay *et al*., 1996) and observed a bias in the UTH derived from NCEP reanalysis. The finding of the studies by Dessler and Davis (2010) motivated the present study to diagnose the forecast from the mesoscale model WRF initialized with the NCEP GDAS analysis fields. The Indian summer monsoon period (June–September) is chosen because during this time the Indian region is highly influenced by mesoscale convective activities. The WRF model is well suited for the range of applications from idealized research to operational forecasting, and has flexibility to accommodate future enhancements. The UTH computed from relative humidity fields is used to evaluate the model performance as compared to the independent estimates of UTH from satellite platform.

Water vapour measurements in the upper troposphere are very limited. *In-situ* measurements from radiosonde and aircraft are inadequate in the spatial and temporal coverage. The radiosonde networks are the main source of water vapour observations, but have limited accuracy in the upper troposphere (e.g. Elliott and Gaffen, 1991; Soden and Lanzante, 1996). In contrast, satellite observations provide greater spatial and temporal coverage. The water vapour channel (5.6–7.2 μm) of the Indian geostationary satellite Kalpana is sensitive to water vapour in the upper troposphere (Thapliyal *et al*., 2011), and is providing high temporal resolution (30 min interval) measurements of the UTH. An advantage of the satellite based UTH with respect to radiosonde measured relative humidity is the high spatial and temporal coverage, especially over the vast oceanic region where radiosonde observations are sparse.

* Correspondence to: M. V. Shukla, Atmospheric Sciences Division, Atmospheric and Oceanic Sciences Group, Space Applications Centre (ISRO), Ahmedabad, 380015, India.
E-mail: munnvinayak@yahoo.com; munnvinayak@sac.isro.gov.in

The purpose of the present study is to compare the UTH computed from the NCEP analysis with the Kalpana derived UTH during the summer monsoon of 2010. This study further examines its impact on the WRF model predicted UTH when initialized with the NCEP analysis. A limited sensitivity study has also been carried out using various physical parameterizations to choose an appropriate parameterization scheme to generate most accurate forecast. The diurnal and seasonal statistics based on comparison of the model analysis/forecast UTH with the satellite observed UTH is generated and examined in detail. The paper is divided in to five sections: Section 2 presents the details of Kalpana-derived UTH used in this study. The details of the design of experiment, WRF model and NCEP analysis used for its initialization are given in Section 3. Section 4 discusses the results of different experiments. The final section presents the conclusion from various comparisons.

2. Satellite data

Kalpana is the first Indian exclusive meteorological geostationary satellite, built by Indian Space Research Organisation (ISRO), and launched in 2002. The Kalpana satellite carries a very high resolution radiometer (VHRR) that takes observations at 30 min intervals in three bands: visible (VIS; 0.55–0.75 μm), thermal infrared window (TIR; 10.5–12.5 μm) and water vapour absorption band (WV; 5.6–7.2 μm). The spatial resolution of the VHRR is 2 km in the VIS and 8 km in the WV and TIR channels at nadir. These observations are used to derive the cloud cover, atmospheric motion vectors, quantitative precipitation estimates, outgoing long wave radiation and UTH. The Kalpana WV channel is sensitive to the relative humidity changes in a broad layer between 200 and 500 hPa with peak sensitivity at ∼325 hPa (Thapliyal *et al*., 2011). The UTH products from Kalpana are generated at 40 km resolution at sub-satellite point (corresponding to the segments of 5×5 pixels) operationally at 30 min. interval and are available from MOSDAC (www.mosdac.gov.in) and the India Meteorological Department (IMD, www.imd.gov.in). It has been found that there are few cases when Kalpana UTH is unavailable for synoptic hours corresponding to the model forecast. A time window of ± 1 h is selected to fill this data gap.

3. Description of the model and experiment

The mesoscale model employed in this study is the Weather Research and Forecasting (WRF; Skamarock *et al*., 2008) model. The WRF is a limited area, non-hydrostatic, primitive equation model with multiple options for various physical parameterization schemes. The present version employs Arakawa C-grid staggering for the horizontal grid and a fully compressible system of equations. The time-split integration uses a third order Runge-Kutta scheme with a smaller time step for acoustic and gravity wave modes. The WRF model physics options used in this study is Kessler (Kessler, 1969), Thompson (Thompson *et al*., 2004) and WRF Single Moment 3-class (WSM3) (Lin *et al*., 1983) for micro-physics schemes; the Kain-Fritsch (KF) scheme (Kain, 2004), Grell (Grell and Devenyi, 2002) and BMJ (Betts and Miller, 1986) for the cumulus convection parameterization scheme, and the Yonsei University (YSU) scheme for planetary boundary layer (Hong and Pan, 1996; Hong and Dudhia, 2003). The Rapid Radiative Transfer Model (RRTM; Mlawer *et al*., 1997) and Dudhia scheme (Dudhia, 1989) were used for long wave and short wave radiation, respectively. All experiments were conducted with single domain (12.1–143.8 °E, 50.8 °S to 50.8 °N) consisting of 295×265 grid points with 50 km horizontal grid resolution. The model has 36 vertical levels with the top of the model atmosphere located at 10 hPa.

The NCEP GDAS analysis available at $1^\circ \times 1^\circ$ spatial resolution is used at a 6 h interval. The NCEP analysis of relative humidity is used to compute the UTH using the weighting function (Thapliyal *et al*., 2011) of the Kalpana water vapour channel. Since Kalpana UTH and NCEP derived UTH are at different spatial resolution, the Kalpana products are re-sampled to the spatial resolution of NCEP analysis using bi-linear interpolation.

For diagnostics of the WRF model forecast UTH, the KF cumulus parameterization and WSM-3 microphysics are used. Four daily experiments have been performed with NCEP analysis as initial and lateral boundary conditions at 0000, 0600, 1200 and 1800 UTC for a 24 h forecast during June–September 2010. The model forecast UTH fields are also re-sampled at $1^\circ \times 1^\circ$ spatial resolution.

4. Result and discussion

The objective of this study is to assess the NCEP analysis and WRF model forecast relative humidity in upper troposphere using Kalpana-derived UTH products over the Indian region during 2010 summer monsoon. The UTH from Kalpana is retrieved only in clear-sky cases, whereas the UTH computed from NCEP belongs to all-sky condition. Therefore, this study is restricted for the comparisons made over the clear-sky cases where observations are available through Kalpana. This kind of evaluation would improve our understanding and ability to predict the various mesoscale phenomena using WRF model initialized with the NCEP analysis. In addition to the initial atmospheric fields, mesoscale models are also sensitive to the physical parameterization. A preliminary sensitivity test has also been carried out for the selection of appropriate combination of the cumulus parameterization and microphysics in the WRF model. Nine experiments have been performed for 3–9 August 2010 based on three different microphysics (Kessler, Thompson and WSM-3) and cumulus parameterization (BMJ, Grell and KF) schemes. Here, bias and root-mean-square-difference (RMSD) are considered as the standard quantification to evaluate the performance of NCEP analysis and WRF model forecast with the Kalpana UTH. The bias and RMSD are defined as:

$$\text{Bias} = \frac{1}{N}\sum_{i=1}^{N}(\text{UTH}_{\text{kalpana}} - \text{UTH}_{\text{NCEP/WRF}}) \quad (1)$$

$$\text{RMSD} = \sqrt{\frac{1}{N}\sum_{i=1}^{N}(\text{UTH}_{\text{kalpana}} - \text{UTH}_{\text{NCEP/WRF}})^2} \quad (2)$$

4.1. Analysis comparisons

Paltridge *et al*. (2009) found that specific humidity in the NCEP/NCAR reanalysis declined between 1973 and 2007, particularly in the tropical mid and upper troposphere. In extension of this study, Dessler and Davis (2010) intercompared various reanalysis fields and suggested that the tropospheric humidity field from NCEP/NCAR reanalysis has

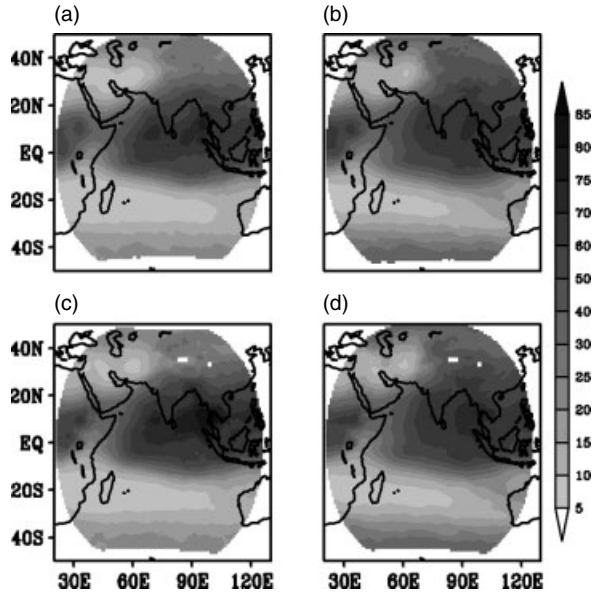

Figure 1. Spatial distribution of mean UTH from (a) Kalpana and (b) NCEP at 0600 UTC and mean UTH from (c) Kalpana and (d) NCEP at 1800 UTC.

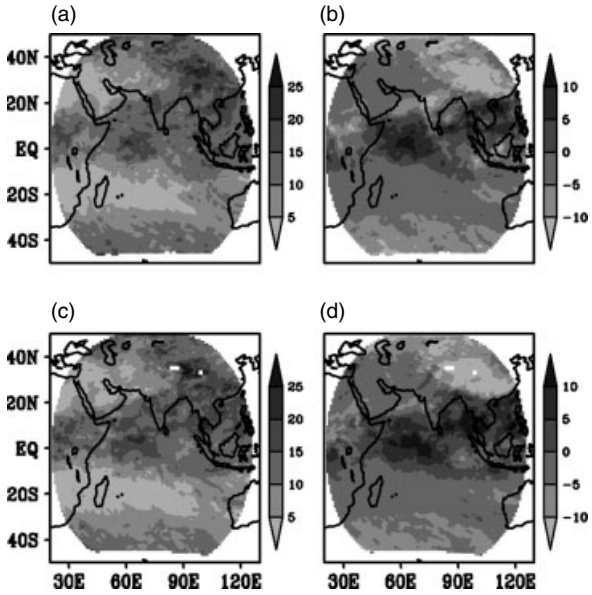

Figure 2. Spatial distribution of (a) RMSD and (b) bias of NCEP analysed UTH with Kalpana UTH at 0600 UTC and (c) RMSD and (d) bias of NCEP analysed UTH with Kalpana UTH at 1800 UTC for June.

a bias. They used tropospheric humidity derived from the Atmospheric Infrared Sounder (AIRS) to show that there are large biases in the NCEP/NCAR reanalysis. Therefore, it is desirable to compare the UTH calculated from NCEP analysis before the model forecast diagnostics. For comparison with the Kalpana observations, the UTH fields are calculated from the NCEP analysis using:

$$\mathrm{UTH} = \frac{\sum_{i=1}^{N} w_i \times \mathrm{RH}_i}{\sum_{i=1}^{N} w_i} \tag{3}$$

where RH is the relative humidity and w is the weight at the level 'i' as shown in the Thapliyal *et al*. (2011). The mean NCEP analysed UTH fields are computed by averaging the UTH values from all the experiments during June–September 2010 (122 days at 0000, 0600, 1200 and 1800 UTC). Comparison of the NCEP analysis is performed at each of the synoptic hours. However, the day (0600 UTC) and night (1800 UTC) time comparisons are specifically shown to highlight the average behaviour of NCEP analysis vis-a-vis Kalpana UTH during day and night time.

Figure 1 shows the seasonal mean UTH (June–September) from the Kalpana observations and NCEP analysis during day and night time. Overall, the Kalpana UTH (Figure 1(a) and (c)) matches well with NCEP UTH (Figure 1(b) and (d)) that captures the low moisture region of the inter-tropical convergence zone (ITCZ) and northern subtropical regions as well as the high moisture regions of the Indian Ocean. However, a few localized regions such as the high moisture region in Arabian Sea and Myanmar are underestimated (∼10%) in the NCEP analysis. This effect is much more prominent during the night time. It may also be inferred from Figure 1 that the NCEP UTH over estimates the low moisture regions, whereas it underestimates the high humidity conditions. Dessler and Davis (2010) also showed the same behaviour in the NCEP reanalysis when compared with the AIRS observation.

The day and night time statistics in terms of RMSD and bias in NCEP UTH with Kalpana UTH are shown in Figure 2. It has been shown in Figure 2 parts (b) and (d) that there is a positive bias in NCEP UTH over the equatorial Indian Ocean and negative bias over other regions. The negative bias is less than 5% in tropical region and more than 10% in the Tibetan high altitude region. The positive bias observed over the Indian Ocean may be due to the following reasons: (1) during the monsoon season the upper troposphere is highly humid because of the prevailing convective process, which the NCEP analysis is not able to capture efficiently and, (2) in the Kalpana observations, due to its inability to detect small cloud contamination, this introduces bias in the UTH estimates. Therefore, there is a possibility that the comparison of the partial-cloud-contaminated UTH from Kalpana with the NCEP analysis might produce high bias in such regions. The large negative bias seen over the high topographic region can be attributed to the effect of high orographic regions on NCEP analysis moisture profiles. Apart from this, the small negative bias may also be attributed to the bias in Kalpana water vapour radiance itself. The weighting function used in this study has fixed vertical pressure co-ordinates. The weighting function shifts due to the vertical temperature variations contribute a small error in the UTH calculations. The high RMSD (> 10%) regions are in concurrence with the regions of high negative or positive biases. As expected, an RMSD of less than 5% is observed over low moisture regions for both day (Figure 2(a)) and night (Figure 2(c)) cases. It is observed from Figure 2 that the low and high biases are intensified in the night time situation in comparison to the day time. The reason for this diurnal variation in bias may be because of the diurnal behaviour of Kaplana-observed water vapour radiances. Thapliyal *et al*. (2010) presented equations to compute Kalpana-derived UTH from WV radiance. It is evident from the equation given therein that for smaller values of WV brightness temperature result in higher values of UTH and *vice versa*. Shukla *et al*. (2012)

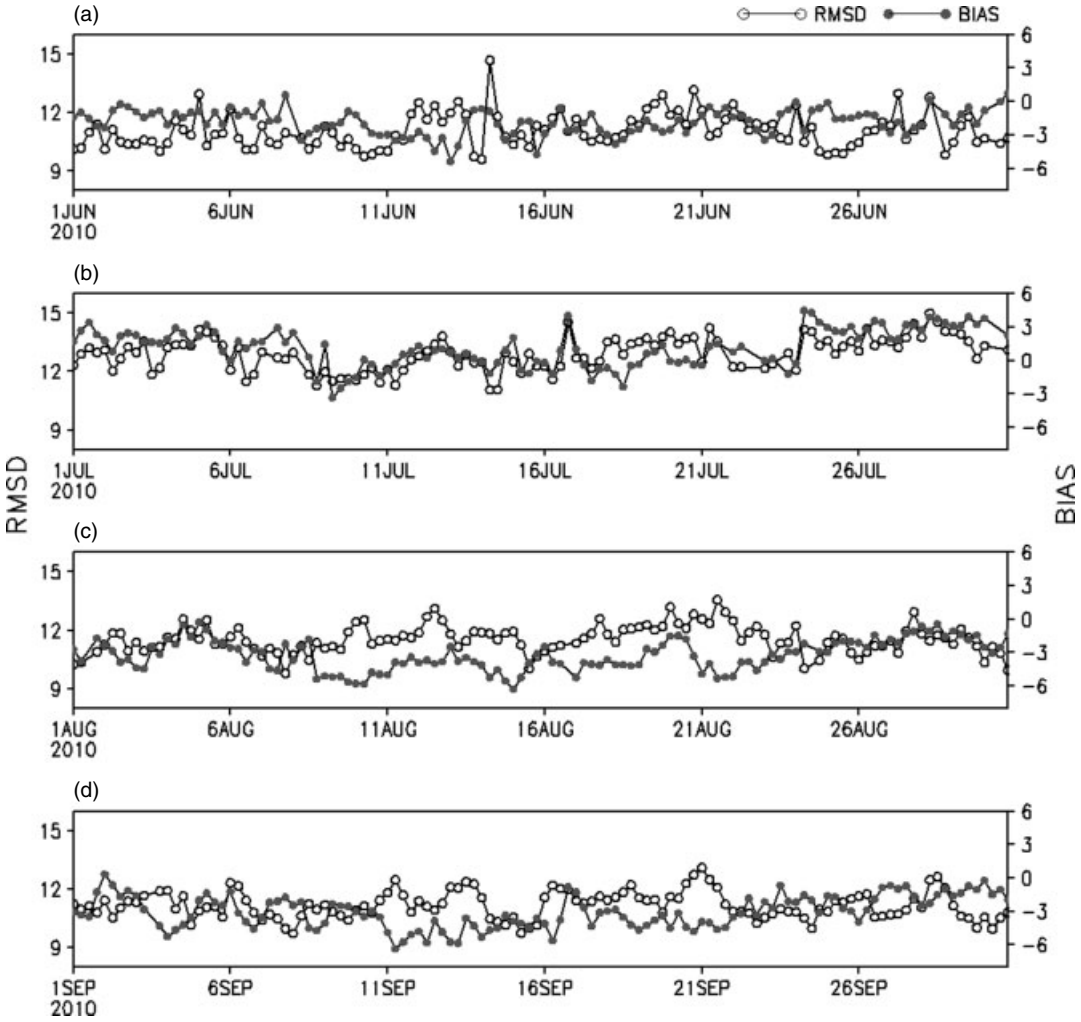

Figure 3. Temporal distribution of RMSD and bias of NCEP analysed UTH for the month of (a) June, (b) July, (c) August and (d) September.

reported diurnal biases in the Kalpana TIR radiances and also provided possible reasons for biases in observed radiances. Similar biases are also observed in Kalpana WV radiances when compared with IASI radiances. This shows that during night time there is larger underestimation in Kalpana-observed WV radiances in comparison to daytime WV radiances. Therefore, values of derived UTH during night time are higher. This is in concurrence with the diurnal variations of the bias in Kalpana UTH (Thapliyal *et al*., 2011). The same kind of results is observed when Kalpana-derived UTH is compared with UTH computed from NCEP analyses. The domain averaged RMSD and bias for the day time are 10.5 and -2.68%, respectively, which slightly decreased to 10.42 and -1.37% in the night time for June. In July, the regions of high RMSD and bias have increased in comparison to other months. Similar features are observed in the RMSD and bias calculation for August. During July and August a high error is observed in the direction of the southwest monsoon flow. This error has reduced with the withdrawal of monsoon in September. The monthly RMSD in UTH for each month is $\sim$10%. Overall, it has been shown that a large variation of the UTH is observed over the Indian region during the summer monsoon period. Therefore, the UTH information obtained from the Kalpana satellite may be crucial to improve the NCEP analysis as the initial condition.

Figure 3 shows the temporal variations of RMSD and bias (domain average) for June–September. An RMSD of $\sim$11% and bias of $\sim -3\%$ is observed in all the 6 h analyses during June (Figure 3(a)). In July, the RMSD in UTH has increased by $\sim$2% in comparison to the RMSD during the previous month. Unlike other months, in July (Figure 3(b)) a positive bias is observed for many days: this is because of the high positive bias over the equatorial region in this month, which is relatively much more extended than other cases. It may be inferred from Figure 3 that the bias and RMSD vary in tandem for high humid cases such as July and the first half of August (Figure 3(c)), i.e. the high RMSD values are mainly driven by the bias. During the weaker phase of the monsoon the RMSD values are in general small and biases are negative.

The scatter plots of monthly mean Kalpana and NCEP analysed UTH during day time are shown in Figure 4. Here, the RMSD is computed from the monthly mean UTH fields considering all the grid-points. An RMSD of less than 10% is observed in the NCEP analysis in comparison to the Kalpana UTH and a high correlation is observed between the two data-sets. In agreement with the previous results, during July (Figure 4(b)) and August (Figure 4(c)) an RMSD of $\sim$7% is observed in the NCEP analysis, which is slightly higher than other 2 months, where the RMSD of $\sim$6% is observed. For all the months, a correlation of $\sim$0.95 is observed, whereas a small inclination towards high UTH values in Kalpana is seen in the month of July. A similar trend and values are also observed in night time comparison. An almost 1% higher RMSD is

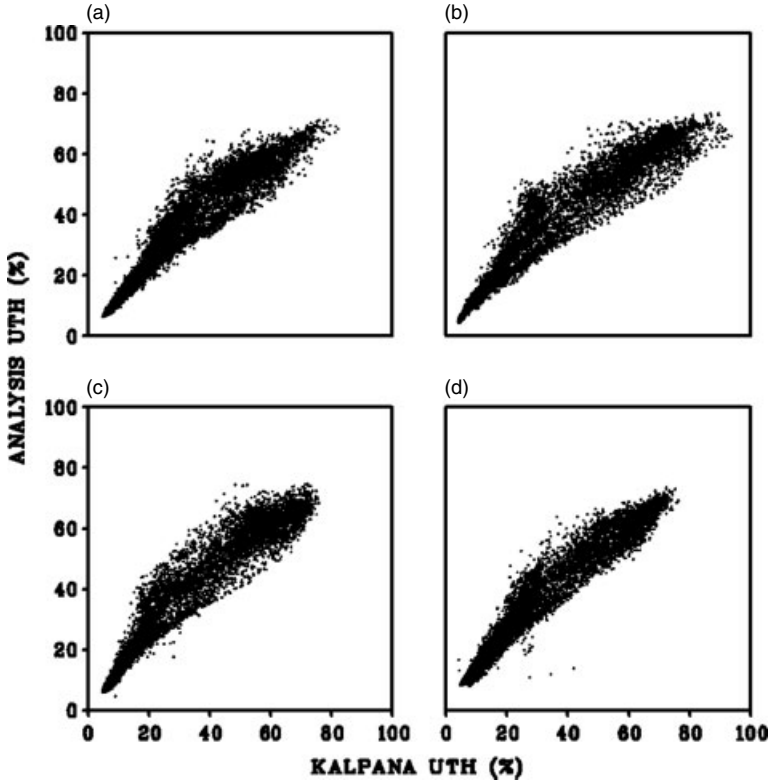

Figure 4. Scatter plot of NCEP analysed UTH with Kalpana UTH for the month of (a) June, (b) July, (c) August and (d) September at 0600 UTC.

observed during night time in comparison to day time RMSD error in the NCEP analysis with the Kalpana UTH, which is higher in the month of July.

4.2. Sensitivity test

This sensitivity study forms a base to show an optimum selection of microphysics and cumulus parameterization schemes for comparing model forecasted UTH fields with satellite derived UTH. The sensitivity test is performed for short duration, and a greater number of cases is required to find the generalized physical option for the WRF model. For this study, a limited sensitivity test has been performed for heavy rainfall case during 3–9 August 2010. This period is considered as it covers the extreme weather event as well as the normal weather conditions. Therefore, it may be assumed that this sensitivity test is valid for the whole period taken in this study. Nine diverse combinations of three microphysics (MP; Kessler, Thompson and WSM-3) and three different cumulus parameterization (CP; BMJ, GRELL and KF) schemes are selected for the study. Figure 5 shows that the nine different combinations of the cumulus parameterization and microphysics options in which 24 h WRF model forecasts are compared with Kalpana UTH. This preliminary sensitivity test shows that the Kessler microphysics and BMJ cumulus parameterization based experiments produced higher RMSD ($> 13\%$) during this period in comparison to other experiments. The WSM-3 microphysics and KF cumulus parameterization shows the minimum RMSD of $\sim 12\%$ out of all other tests but it has a slightly higher bias in comparison to the experiment when the Grell scheme is used. This test is a limited case study and many diverse cases for many years are required to arrive at any concrete conclusion. However, in this study, a suitable scheme on the basis of smallest RMSD and higher correlation was selected (Table 1). Therefore, the WSM-3 and KF schemes are used for microphysics and cumulus parameterizations for further experiments.

4.3. Forecast comparison

In this section, the UTH computed from the WRF model forecast when initialized from the NCEP analysis is validated with the Kalpana UTH for synoptic hours (0000, 0600, 1200 and 1800 UTC). On the basis of the sensitivity test, KF cumulus parameterization and WSM-3 microphysics schemes have been chosen for all the experiments. Four daily forecast experiments are performed during June to September (122 days), 2010. The RMSD and biases are calculated separately at day and night time to see the diurnal variations of the errors in forecast UTH. The temporal distribution of daily and spatially average RMSD and bias are calculated for model forecast UTH. Figure 6 shows the temporal distribution of bias and RMSD in 12 and 24 h forecast UTH. From Figure 6 it is evident that there is a negative bias during the whole period except in July, in which the bias is positive. It is also observed that for most of the period the daytime bias in both 12 and 24 h forecasts are smaller than the night time bias. The errors in model forecast UTH are attributed to the uncertainties in initial condition, parameterization and model errors. In the present study, the error in model forecast UTH follows similar pattern as observed in UTH derived from NCEP analysis. The impact of uncertainties in initial conditions on NWP model forecast is discussed by Rabier *et al*. (1996). The effect of departure in NCEP analysis-derived UTH (Figure 3) are reflected in the subsequent WRF model forecast for all simulation periods (Figure 6). A negative bias is observed in the NCEP analysis for June, August and September, which further intensifies in subsequent 12 and 24 h forecasts for the same period.

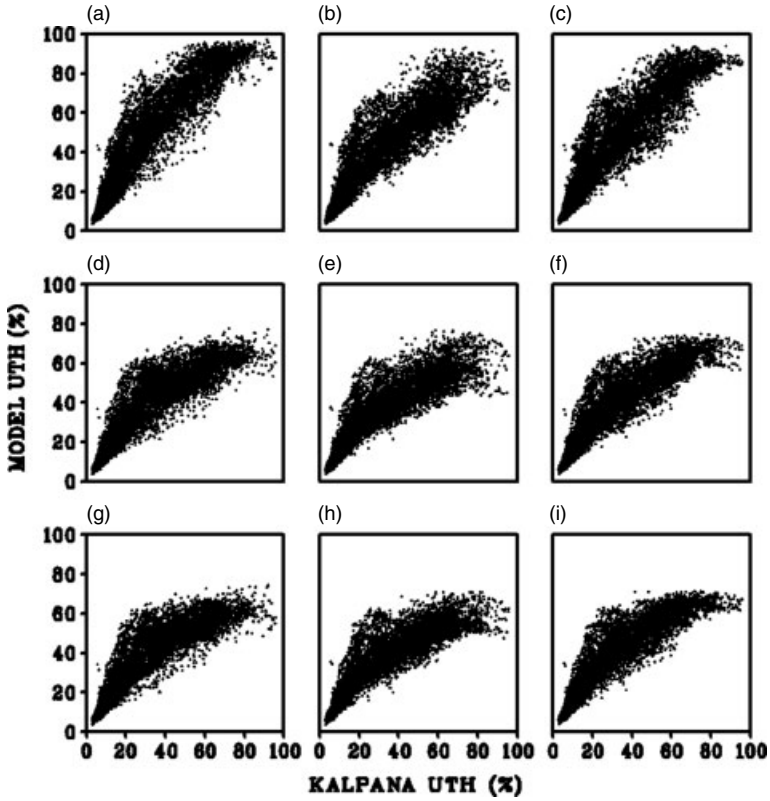

Figure 5. Scatter plot of 24 h forecasted UTH with Kalpana observed UTH for (a) Kesler and BMJ (b) Kesler and Grell (c) Kesler and KF (d) Thompson and BMJ (e) Thompson and Grell (f) Thompson and KF (g) WSM and BMJ (h) WSM and Grell and (i) WSM and KF nine different combinations of parameterization schemes at 0600 UTC.

Table 1. Error Statistics of 24-h UTH forecast.

WRF Physics	BMJ CP	GRELL CP	KF CP
Kesler MP	BIAS = −12.1% RMSD = 18.6% Corr = 0.77	BIAS = −6.9% RMSD = 14.7% Corr = 0.68	BIAS = −9.1% RMSD = 15.7% Corr = 0.74
THOMPSON MP	BIAS = −4.4% RMSD = 13.4% Corr = 0.73	BIAS = −2.6% RMSD = 13.5% Corr = 0.67	BIAS = −4.4% RMSD = 13.0% Corr = 0.72
WSM-3 MP	BIAS = −4.1% RMSD = 13.0% Corr = 0.76	BIAS = −2.6% RMSD = 13.0% Corr = 0.71	BIAS = −4.6% RMSD = 12.7% Corr = 0.77

Similarly, a positive bias for July contributes to a positive bias in the 12 and 24 h forecasts. During the entire period a smaller RMSD is observed in the day time (0600 UTC) in comparison to night time (1800 UTC). For all days, the RMSD of ∼12 and ∼13% were observed in 12 and 24 h forecasts, respectively, which is ∼2% higher in July. In contrast to the other months, night time RMSD is higher than the daytime RMSD in July. The difference of RMSD for day and nighttime forecast UTH is small for June, August and September.

Figure 7 shows the scatter diagram of the monthly mean 24 h model predicted and the Kalpana UTH during June–September for the daytime comparison. The RMSD and bias of about 7 and −3.45% respectively are observed in the 24 h forecast UTH (Figure 7(a)) for June and shows a 95% correlation with the Kalpana UTH. In July (Figure 7(b)) and August (Figure 7(c)) the RMSD in forecast UTH has increased by ∼1% in comparison to that of June. In September (Figure 7(d)) the RMSD in forecast UTH has reduced with withdrawal of summer monsoon. The RMSD of ∼8% is observed during night time, which is higher in July (∼10%).

5. Conclusion

In the present study, the upper tropospheric humidity (UTH) derived from the Indian geostationary satellite Kalpana is used for the diagnostic study of the WRF model forecast over the Indian domain and also to evaluate the quality of the initial condition that is taken from the NCEP analysis. The UTH computed from the NCEP analysis and WRF model forecast is compared with the Kalpana UTH for the months of June–September 2010, a normal monsoon year. The spatial and

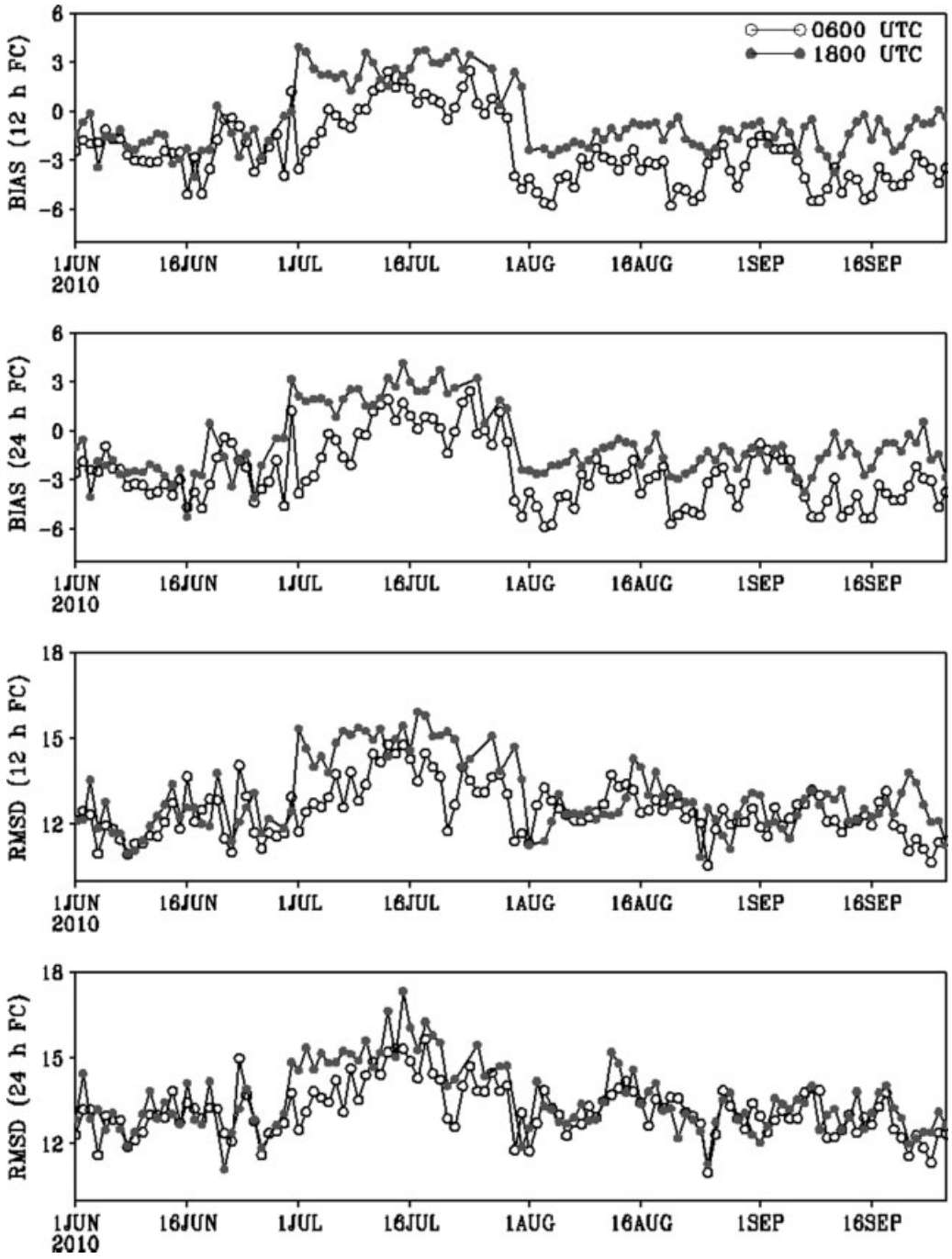

Figure 6. Temporal distribution of Bias and RMSD for 12 and 24 h predicted UTH valid at 0600 and 1800 UTC during June–September.

temporal variation in NCEP UTH and Kalpana UTH matches very well and show the same features. The same pattern shown in Kalpana UTH and NCEP UTH proves that the NCEP analysed fields are able to capture the low and high moisture regions in the upper troposphere. However, the NCEP UTH has some bias with respect to Kalpana UTH which is higher in July. The bias and root-mean-square-difference (RMSD) is not constant spatially but both the NCEP analysed and model forecast UTH underestimate in the convective regions, whereas they overestimate in other regions compared to the Kalpana UTH. As expected, the bias and RMSD increased in model forecast UTH in comparison to NCEP analysed UTH. The sensitivity analysis of the model gave an insight to use the WSM-3 microphysics and KF cumulus parameterization schemes over Indian region for short term moisture forecast. The model forecast UTH is generated by using the same parameterization scheme and NCEP analysed fields as initial conditions. The Weather Research and Forecasting (WRF) mesoscale model forecast UTH also follows the similar spatial and temporal distribution as captured by the NCEP analysis, but with a higher RMSD and bias.

Acknowledgements

The authors would like to thank Dr. A. S. Kiran Kumar, Director, SAC and Dr. J. S. Parihar, Deputy Director, EPSA/SAC for constant encouragement and guidance. Authors are thankful to National Center for Atmospheric Research (NCAR) for WRF

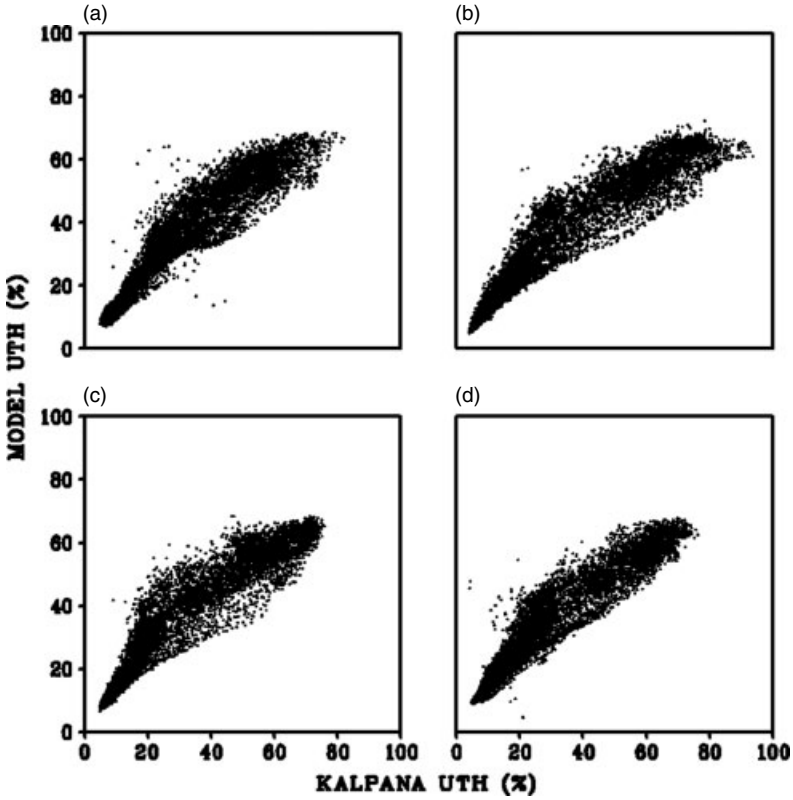

Figure 7. Scatter plot of 24 h forecasted UTH with Kalpana UTH for the month of (a) June, (b) July, (c) August and (d) September at 0600 UTC.

Model and the analysis. The global analysed data provided by National Centers for Environmental Prediction (NCEP) are acknowledged with sincere thanks. The authors would like to thank MOSDAC for providing Kalpana products.

References

Bates JJ, Wu X, Jackson DL. 1996. Interannual variability of upper-tropospheric water vapour band brightness temperature. *J. Clim.* **9**: 427–438.

Betts AK, Miller MJ. 1986. A new convective adjustment scheme. Part II: single column tests using GATE wave, BOMEX, and arctic air-mass data sets. *Q. J. R. Meteorol. Soc.* **112**: 693–709.

Blackwell KG, McGuirk MP. 1996. Tropical upper-tropospheric dry regions from TOVS and radiosondes. *J. Appl. Meteorol.* **35**: 464–481.

Brown RG, Zhang C. 1997. Variability of midtropospheric moisture and its effect on cloud top height distribution during TOGACOARE. *J. Atmos. Sci.* **54**: 2760–2774.

Clark HL, Harwood RS. 2003. Upper tropospheric humidity from MLS and ECMWF reanalysis. *Mon. Weather Rev.* **131**: 542–555.

Dessler AE, Davis SM. 2010. Trends in tropospheric humidity from reanalysis systems. *J. Geophys. Res.* **115**: D19127, DOI: 10.1029/2010JD014192.

Dudhia J. 1989. Numerical study of convection observed during the winter monsoon experiment using a mesoscale two-dimensional model. *J. Atmos. Sci.* **46**: 3077–3107.

Elliott WP, Gaffen DJ. 1991. On the utility of radiosonde humidity archives for climate studies. *Bull. Am. Meteorol. Soc.* **72**: 1507–1520.

Grell GA, Devenyi D. 2002. A generalized approach to parameterizing convection combining ensemble and data assimilation techniques. *Geophys. Res. Lett* **29**(14): 4, Article 1693.

Hong SY, Dudhia J. 2003. Testing of a new non-local boundary layer vertical diffusion scheme in Numerical weather prediction applications. *20th Conference on Weather Analysis and Forecasting/16th Conference on Numerical Weather Prediction*, Seattle, WA.

Hong SY, Pan HL. 1996. Nonlocal boundary layer vertical diffusion in a medium range forecast model. *Mon. Weather Rev.* **124**: 2322–2339.

Kain JS. 2004. The Kain-Fritsch convective parameterization: an update. *J. Appl. Meteorol.* **43**: 170–181.

Kalnay E, Kanamitsu M, Kistler R, Collins W, Deaven D, Gandin L, Iredell M, Saha S, White G, Woollen J, Zhu Y, Leetmaa A, Reynolds R, Chelliah M, Ebisuzaki W, Higgins W, Janowiak J, Mo KC, Ropelewski C, Wang J, Jenne R, Joseph D. 1996. The NCEP/NCAR 40 year reanalysis project. *Bull. Am. Meteorol. Soc.* **77**: 437–471.

Kessler E. 1969. On the distribution and continuity of water substance in atmospheric circulation. *Meteorol. Monogr. (Am. Meteorol. Soc.)* **32**: 84.

Lamquin N, Gierens K, Stubenrauch CJ, Chatterjee R. 2008. Evaluation of upper tropospheric humidity forecasts from ECMWF using AIRS and CALIPSO data. *Atmos. Chem. Phys. Discuss.* **8**: 17907–17937.

Lin YL, Farley RD, Orville HD. 1983. Bulk parameterization of the snow field in a cloud model. *J. Clim. Appl. Meteorol.* **22**: 1065–1092.

McNally AP, Vesperini M. 1996. Variational analysis of humidity information from TOVS radiances at ECMWF. *Q. J. R. Meteorol. Soc.* **122**: 1521–1544.

Macpherson B, Wright BJ, Hand WH, Maycock AJ. 1996. The impact of MOPS moisture data in the U. K. Meteorological Office mesoscale data assimilation scheme. *Mon. Weather Rev.* **124**: 1746–1766.

Mlawer EJ, Taubman SJ, Brown PD, Iacono MJ, Clough SA. 1997. Radiative transfer for inhomogeneous atmosphere: RRTM, a validated correlated-k model for the longwave. *J. Geophys. Res.* **102**(D14): 16663–16682.

Onogi K, Tsutsui J, Koide H, Sakamoto M, Kobayashi S, Hatsushika H, Matsumoto T, Yamazaki N, Kamahori H, Takahashi K, Kadokura S, Wada K, Kato K, Oyama R, Ose T, Mannoji N, Taira R. 2007. The JRA-25 reanalysis. *J. Meteorol. Soc. Jpn.* **85**: 369–432.

Paltridge G, Arking A, Pook M. 2009. Trends in middle- and upper-level tropospheric humidity from NCEP reanalysis data. *Theor. Appl. Climatol.* **98**: 351–359.

Rabier F, Klinker E, Courtier P, Hollingsworth A. 1996. Sensitivity of forecast errors to initial conditions. *Q. J. R. Meteorol. Soc.* **122**: 121–150.

Salathé EP, Chesters D, Sud YC. 1995. Variability of moisture in the upper-troposphere as inferred from TOVS satellite observations and the ECMWF model analysis in 1989. *J. Clim.* **8**: 120–132.

Schmetz J, Berg LVD. 1994. Upper Tropospheric Humidity observations from Meteosat compared with short-term forecast fields. *Geophys. Res. Lett.* **21**(7): 573–576.

Shukla MV, Thapliyal PK, Bisht JH, Mankad KN, Pal PK, Navalgund RR. 2012. Intersatellite calibration of Kalpana thermal infrared channel using AIRS hyperspectral observations. *IEEE Geosci. Remote. Sens. Lett.* **9**: 687–689.

Simmons A, Uppala S, Dee D, Kobayashi S. 2007. ERA-Interim: new ECMWF reanalysis products from 1989 onwards. *ECMWF Newslett.* **110**: 1–53.

Skamarock WC, Klemp JB, Dudhia J, Gill DO, Barker DM, Duda MG, Huang XY, Wang W, Powers JG. 2008. *A Description of the Advanced Research WRF Version 3*. NCAR Technical Note NCAR/TN-475 STR. Mesoscale and Microscale Meteorology Division, National Center of Atmospheric Research: Boulder, CO; 113 pp.

Soden BJ, Bretherton FP. 1993. Upper tropospheric relative humidity from GOES 6.7 μm channel: method and climatology for July 1987. *J. Geophys. Res.* **98**: 16669–16688.

Soden BJ, Fu R. 1995. A satellite analysis of deep convection, upper tropospheric humidity and the greenhouse effect. *J. Clim.* **8**: 2333–2351.

Soden BJ, Lanzante JR. 1996. An assessment of satellite and radiosonde climatologies of upper-tropospheric water vapour. *J. Clim.* **9**: 1235–1250.

Suarez MJ, Rienecker MM, Suarez MJ, Todling R, Bacmeister J, Takacs L, Liu HC, Gu W, Sienkiewicz M, Koster RD, Gelaro R, Stajner I, Nielsen JE. 2008. The GEOS-5 Data Assimilation System – Documentation of versions 5.0. 1, 5.1.0, and 5.2.0, NASA Tech. Memo., NASA/TM-2008-104606. Vol. 27; 97 pp.

Thapliyal PK, Shukla MV, Shah S, Joshi PC, Pal PK, Ajil KS. 2011. An algorithm for the estimation of upper tropospheric humidity from Kalpana observations: methodology and validation. *J. Geophys. Res* **116**: D01108, DOI: 10.1029/2010JD014291.

Thompson G, Rasmussen RM, Manning K. 2004. Explicit forecasts of winter precipitation using an improved bulk microphysics scheme. Part I: description and sensitivity analysis. *Mon. Weather Rev.* **132**: 519–542.

Uppala S, Kallberg PW, Simmons AJ, Andrae U, Bechtold VDC, Fiorino M, Gibson JK, Haseler J, Hernandez A, Kelly GA, Li X, Onogi K, Saarinen S, Sokka N, Allan RP, Andersson E, Arpe K, Balmaseda MA, Beljaars ACM, Berg LVD, Bidlot J, Bormann N, Caires S, Chevallier F, Dethof A, Dragosavac M, Fisher M, Fuentes M, Hagemann S, Hólm E, Hoskins BJ, Isaksen L, Janssen PAEM, Jenne R, Mcnally AP, Mahfouf JF, Morcrette JJ, Rayner NA, Saunders RW, Simon P, Sterl A, Trenberth KE, Untch A, Vasiljevic D, Viterbo P, Woollen J. 2005. The ERA-40 re-analysis. *Q. J. R. Meteorol. Soc.* **131**: 2961–3012.

